AGU PUBLICATIONS

Geophysical Research Letters

RESEARCH LETTER

10.1002/2017GL076872

Key Points:

- Depleted and less metasomatic MORB mantle fed the late Oligocene seafloor spreading of the South China Sea
- MORBs and OIBs of the South China Sea record a Miocene MORB mantle enrichment and possibly signal contributions of the Hainan Plume

Supporting Information:

- Supporting Information S1
- Data Set S1

Correspondence to:
Y. Yan,
yanyi@gig.ac.cn

Citation:
Yu, M., Yan, Y., Huang, C.-Y., Zhang, X., Tian, Z., Chen, W.-H., & Santosh, M. (2018). Opening of the South China Sea and upwelling of the Hainan plume. *Geophysical Research Letters*, *45*, 2600–2609. https://doi.org/10.1002/2017GL076872

Received 19 DEC 2017
Accepted 28 FEB 2018
Accepted article online 5 MAR 2018
Published online 22 MAR 2018

Opening of the South China Sea and Upwelling of the Hainan Plume

Mengming Yu[1,2], Yi Yan[1], Chi-Yue Huang[1,3,4], Xinchang Zhang[1], Zhixian Tian[1], Wen-Huang Chen[1], and M. Santosh[5,6,7]

[1]Key Laboratory of Ocean and Marginal Sea Geology, Guangzhou Institute of Geochemistry, Chinese Academy of Sciences, Guangzhou, China, [2]College of Earth and Planetary Sciences, University of Chinese Academy of Sciences, Beijing, China, [3]School of Ocean and Earth Science, Tongji University, Shanghai, China, [4]Department of Earth Sciences, National Cheng Kung University, Tainan, Taiwan, [5]School of Earth Sciences and Resources, China University of Geosciences, Beijing, China, [6]Department of Earth Sciences, University of Adelaide, Adelaide, Australia, [7]Department of Geology, Northwest University, Xi'an, China

Abstract Opening of the South China Sea and upwelling of the Hainan Plume are among the most challenging issues related to the tectonic evolution of East Asia. However, when and how the Hainan Plume affected the opening of the South China Sea remains unclear. Here we investigate the geochemical and isotopic features of the ~25 Ma mid-ocean ridge basalt (MORB) in the Kenting Mélange, southern Taiwan, ~16 Ma MORB drilled by the IODP Expedition 349, and ~9 Ma ocean island basalt-type dredged seamount basalt. The ~25 Ma MORBs reveal a less metasomatic depleted MORB mantle-like source. In contrast, the Miocene samples record progressive mantle enrichment and possibly signal the contribution of the Hainan Plume. We speculate that MORBs of the South China Sea which could have recorded plume-ridge source mixing perhaps appear since ~23.8 Ma. On the contrary, the Paleocene-Eocene ocean island basalt-type intraplate volcanism of the South China continental margin is correlated to decompression melting of a passively upwelling fertile asthenosphere due to continental rifting.

Plain Language Summary The upwelling of mantle plume can assist continental breakup and seafloor spreading. Opening of the South China Sea and upwelling of the Hainan Plume are among the most challenging issues related to the tectonic evolution of East Asia. However, whether the upwelling of Hainan Plume had contributed to the opening of the South China Sea remains unclear. In this research, we investigate the geochemical and isotopic features of late Oligocene and middle Miocene mid-ocean ridge basalts of the South China Sea. We find the middle Miocene mid-ocean ridge basalts record progressive mantle enrichment and possibly signal the contribution of the Hainan Plume. Integrating with other tectonics, we speculate that the head of Hainan Plume impinged the lithosphere of the South China continental margin at the middle Oligocene, and the arriving of Hainan Plume has contributed to the latest Oligocene/earliest Miocene ridge jump and propagation. On the contrary, the Paleocene and Eocene ocean island basalt-type volcanism in South China continental margin was derived from the passively upwelling of enriched asthenosphere due to continental rifting. This finding can contribute to a better understanding on roles of a starting mantle plume in continental breakup and seafloor spreading.

1. Introduction

The upwelling of mantle plumes can assist continental breakup, particularly in the disaggregation of supercontinents as in the case of the Gondwanaland (Storey, 1995) and preferentially along existing extensional zones, such as the Atlantic (Hill, 1991). The opening of South China Sea has long been correlated to continental breakup and southward drifting of the Palawan-Reed Bank microcontinent from the South China continental margin (Briais et al., 1993; Ru & Pigott, 1986; Taylor & Hayes, 1983) (Figure 1a). Significant volumes of ocean island basalt (OIB)-type intraplate volcanism is developed in the South China continental margin since the late Paleocene (Chung et al., 1994, 1995, 1997; Ho et al., 2000, 2003; X. L. Huang et al., 2013; X. Li et al., 2015; E. Liu et al., 2017; Tu et al., 1992; K. L. Wang, Chung, et al., 2012; K. L. Wang, Lo, et al., 2012; X. C. Wang et al., 2012; X. J. Wang et al., 1985; P. Yan et al., 2006; Q. Yan et al., 2014; Zeng et al., 2017; Zhou et al., 2009; Zhu et al., 2004; H. B. Zou et al., 2000; H. P. Zou et al., 1995) (Figure 1a). Meanwhile, voluminous Paleocene and Eocene island arc basalt (IAB)-type volcanism also developed (Chung et al., 1997; X. L. Huang et al., 2013; K. L. Wang, Chung, et al., 2012; Zhu et al., 2004; H. P. Zou et al., 1995). However, the

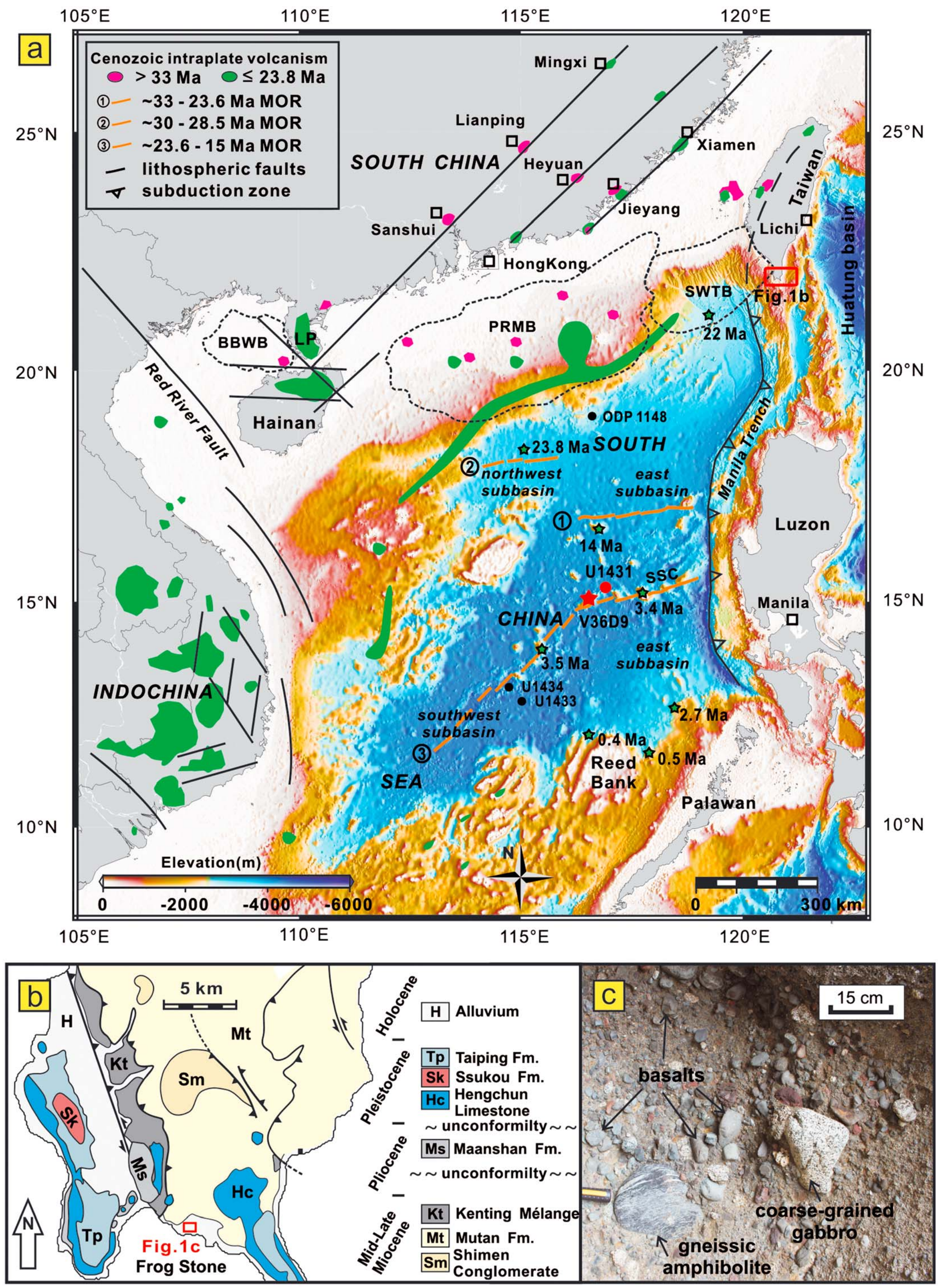

Figure 1. (a) Tectonic sketch map of the area around the South China Sea (after Chung et al., 1997). BBWB = Beibuwan basin; LP = Leizhou Peninsula; MOR = mid-ocean ridge; PRMB = Pearl River Mouth basin; SSC = Scarborough seamount chain; SWTB = Southwest Taiwan basin. The stars show the seamounts with ages. The solid dots depict IODP/ODP drilling sites. The data reported in this study are shown in red star, dot, and rectangle. Distribution of Cenozoic intraplate volcanism is according to Chung et al. (1997), X. L. Huang et al. (2013), X. Li et al. (2015), K. L. Wang, Chung, et al. (2012), K. L. Wang, Lo, et al. (2012), and P. Yan et al. (2006). (b) Geological map of the Hengchun Peninsula, southern Taiwan (after X. Zhang et al., 2016). (c) Photograph of conglomerates on the Frog Stone beach.

OIB-type intraplate volcanism of the South China continental margin paused during the Oligocene but resumed since the earliest Miocene and reached a peak during late Pliocene and early Pleistocene (X. L. Huang et al., 2013; Y. G. Xu et al., 2012; P. Yan et al., 2006; Zhu et al., 2004). Recent studies identified the Hainan Plume based on seismic imaging (Lebedev & Nolet, 2003; Lei et al., 2009; S. Wei & Chen, 2016), and the existence of this plume is supported by petrologic and geochemical evidence from the late Cenozoic Hainan flood basalts (X. C. Wang et al., 2012; Wang et al., 2013). Furthermore, the late Cenozoic OIB-type intraplate volcanism in the South China Sea and the Indochina region (Figure 1a) are thought to be the products of the Hainan Plume (Wang et al., 2013; Q. Yan et al., 2018). However, the time of birth of the Hainan Plume is less constrained. Several workers have attempted to correlate the Paleocene and Eocene OIB-type intraplate volcanism of the South China continental margin (Figure 1a) to the Hainan Plume (E. Liu et al., 2017; Q. Yan et al., 2014; Zhou et al., 2009). Thus, the opening of the South China Sea may record an example of the interaction between a mantle plume and the rifting-seafloor spreading system developed upon a continental margin.

In order to evaluate the contribution of the upwelling of the Hainan Plume to the opening of the South China Sea, we investigate the geochemical features including Sr, Nd, and Hf isotopes of representative rock types including (1) ~25 Ma amphibolite (Kt9) and basalt cobbles (Kt1, Kt2, and Kt5) collected from the Kenting Mélange, southern Taiwan, which are considered to be the fragments of the South China Sea oceanic crust (Pelletier & Stephan, 1986; X. Zhang et al., 2016); (2) ~16 Ma mid-ocean ridge basalt (MORB) (U1431) collected at site U1431 during IODP Expedition 349 (C. F. Li et al., 2014); and (3) ~9 Ma basalt (V36D9) dredged from the Scarborough seamount chain (X. J. Wang et al., 1985). We integrate our new results with published geochemical data to address the following points: (1) when did the Hainan Plume initiate and (2) the mantle evolution associated with the opening of the South China Sea.

2. Geologic Background

The South China Sea lies at the junction of the Indo-Australian, Pacific, and Eurasian plates, incorporating the east, northwest, and southwest subbasins (Figure 1a). The initial opening of the South China Sea is considered to have involved rifting of an ancient Andean-type continental margin during the latest Cretaceous or early Paleocene (Ru & Pigott, 1986; Taylor & Hayes, 1983). Continental breakup and seafloor spreading occurred during the early Oligocene (~33 Ma, C. F. Li et al., 2014; ~32 Ma; Briais et al., 1993; Taylor & Hayes, 1983) in the east and northwest subbasins. Subsequently, the ridge jumped southward and seafloor spreading propagated into the southwest subbasin at ~23.6 Ma (C. F. Li et al., 2014). Several tectonic models have been proposed for this region including the withdrawal of the subducted Paleo-Pacific Plate (Shi & Li, 2012; Taylor & Hayes, 1983), the tectonic extrusion of Indochina due to India-Eurasian collision (Briais et al.,1993; Tapponnier et al., 1982), slab pull and subduction of the proto-South China Sea under the Sabah/Borneo (Morley, 2002; Taylor & Hayes, 1983), and the extension related to an upwelling mantle plume (Q. Yan et al., 2014; Zhou et al., 2009). The seafloor spreading of the South China Sea terminated at ~16 ± 1 Ma (Briais et al., 1993; C. F. Li et al., 2014; Taylor & Hayes, 1983) and the east subbasin subducted eastward along the Manila Trench (Lallemand et al., 2001; Shao, 2015). Thereafter, the Manila Trench progressively retreated westward and the northern Luzon Arc collided with the South China continent at ~6.5 Ma (C. Y. Huang et al., 1997). The late Miocene Kenting Mélange (Figure 1b) consists of disrupted turbidite layers and large volume of allochthonous basaltic rocks, which is exposed within the Hengchun Peninsula, South Taiwan (C. Y. Huang et al., 1997; X. Zhang et al., 2014). Previous studies proposed that these allochthonous basaltic rocks were scraped off from the South China Sea oceanic lithosphere as a result of subduction of the South China Sea and following arc-continent collision (Pelletier & Stephan, 1986; X. Zhang et al., 2016). Fragments of the Kenting Mélange are exposed on the Frog Stone beach (X. Zhang et al., 2016), which are composed of turbiditic sands and angular-subrounded pebbles/cobbles of gabbro, basalt/diabase, and amphibolite (Figure 1c).

3. Analytical Methods

Samples were initially crushed into small fragments about 1 cm in diameter. Grains with little weathering and no visible secondary minerals were washed with 3% HCl for 15 min and with deionized water several times in a supersonic bath. Leached grains were dried and pulverized using a tungsten carbide mortar into 200 mesh powders. The whole-rock geochemical analyses were conducted at the Guangzhou Institute of Geochemistry, Chinese Academy of Sciences. Analyses of the major oxides and trace elements were

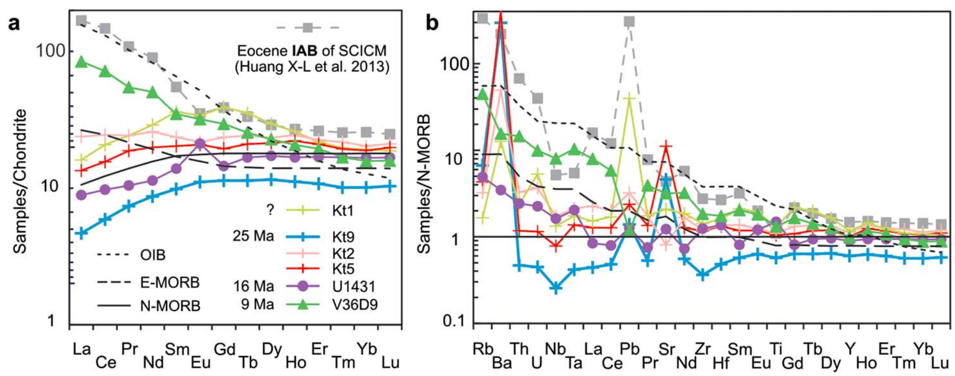

Figure 2. (a) Chondrite-normalized rare Earth element patterns. (b) Normal mid-ocean ridge basalt (N-MORB)-normalized incompatible elements spider diagram. Eocene island arc basalt (IAB) of the South China-Indochina continental margin (SCICM) from X. L. Huang et al. (2013). The chondrite, N-MORB, enriched-MORB (E-MORB), and ocean island basalt (OIB) are from Sun and McDonough (1989).

conducted using a Rigaku ZSX100e X-ray fluorescence spectrometer and a Perkin-Elmer Sciex ELAN 6000 inductively coupled plasma mass spectrometer, respectively. Analytical uncertainties are less than 5% for major oxides and 6% for trace elements in most cases (Table S1). Detailed analytical procedures were given in X. H. Li et al. (2006) and Y. Liu (1996). Measurement of the Sr-Nd-Hf isotopic ratios was performed using a Neptune Plus multicollector inductively coupled plasma mass spectrometer. The analytical procedures were similar to those reported in G. Wei et al. (2002). Sr-Nd-Hf isotopic fractionations were corrected to $^{86}Sr/^{88}Sr$ = 0.1194, $^{146}Nd/^{144}Nd$ = 0.7219, and $^{179}Hf/^{177}Hf$ = 0.7325, respectively. The measured isotope ratios of NBS987, JNdi-1, and JMC14374 standard materials are $^{87}Sr/^{86}Sr$ = 0.710257 ± 0.000013 (2σ, n = 11), $^{143}Nd/^{144}Nd$ = 0.512101 ± 0.000005 (2σ, n = 18), and $^{176}Hf/^{177}Hf$ = 0.282182 ± 0.000006 (2σ, n = 8), respectively. The dissolved sample powders were leached using 6 mol/L distilled HCl following the procedures of Weis et al. (2005). To evaluate the effect of weathering and metasomatism on samples within the Kenting Mélange, Sr-Nd-Hf isotopic analysis of a portion of unleached samples were also conducted. Since the intensity of $^{143}Nd/^{144}Nd$ of the leached Kt5 and $^{176}Hf/^{177}Hf$ of the leached Kt9 is too low to be measured, the Nd and Hf isotopes of unleached counterparts are used. The detailed explanations are presented in the supporting information Table S3.

4. Petrography and Geochemistry

4.1. Igneous Fragments Within the Kenting Mélange, Southern Taiwan

The gneissic amphibolites within the Kenting Mélange are composed of irregularly spaced discontinuous streaks of white plagioclase and dark brownish-black amphibole (Figure 1c). The amphibolite Kt9 consists of plagioclase, hornblende, and ilmenite with a sheared porphyroid texture (Figure S1), which corresponds to amphibolite-facies metamorphism of a gabbroic protolith. Whole-rock geochemical analysis shows that the amphibolite Kt9 has high concentrations of SiO_2 (55.13 wt. %) and Na_2O (5.15 wt. %) compared to gabbros (Figure S2 and Table S2). The total rare earth element (REE) content of the Kt9 is somewhat low. Light rare earth elements (LREEs) are depleted, and the heavy REEs show flat pattern, with a chondrite-normalized $(La/Yb)_N$ value of 0.5 and a $(Dy/Yb)_N$ value of 1.1, which are similar to those of normal MORB (N-MORB) (Sun & McDonough, 1989) (Figure 2a). The rock displays enrichment in large ion lithophile elements (LILEs), such as Rb, Ba, Pb, and Sr, and exhibits clear negative Nb and Zr anomalies relative to the N-MORB (Figure 2b). The sample also shows high $^{87}Sr/^{86}Sr$ (0.70951), $^{143}Nd/^{144}Nd$ (0.51311), and $^{176}Hf/^{177}Hf$ (0.28323). The high ε_{Nd}(t) and ε_{Hf}(t) values are close to those of depleted MORB mantle (DMM) end-member (Figure 3), suggesting that the Nd and Hf isotopes in this rock were not significantly disturbed by the amphibolite-facies metamorphism.

The basalts Kt1, Kt2, and Kt5 show porphyritic to hyalopilitic textures. The samples comprise mainly weathered tabular feldspar phenocrysts and small acicular feldspar crystallites in a cryptocrystalline matrix (Figure S1). The major element compositions of these basalts show marked variation, with high values of loss on ignition (4.1–8.9) (Figure S2 and Table S2). The chondrite-normalized REE pattern, N-MORB-normalized incompatible elements distribution, and Sr-Nd-Hf isotopes of the basalt sample Kt5 are similar to those of

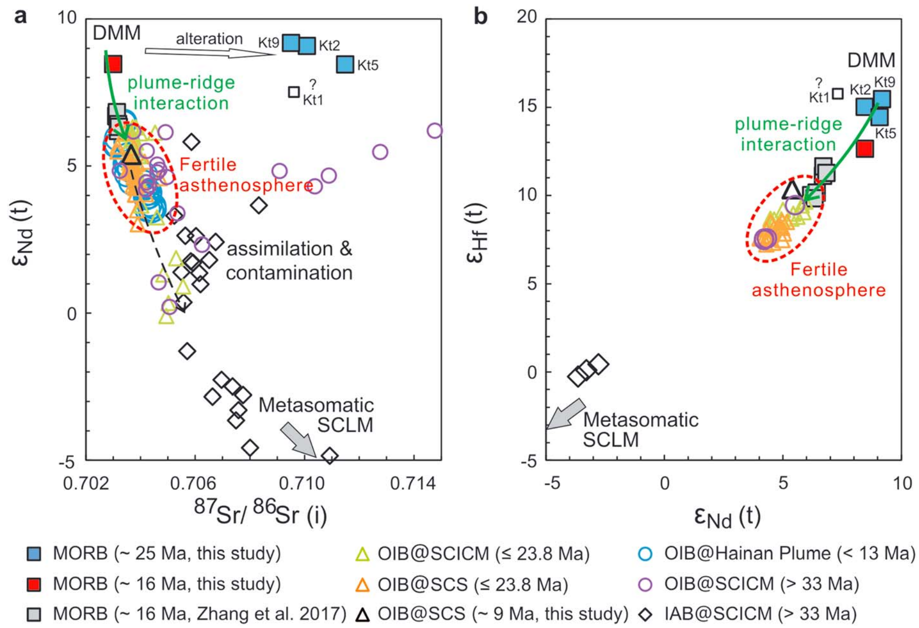

Figure 3. (a) $^{87}Sr/^{86}Sr$ (i) versus ε_{Nd} (t) and (b) ε_{Nd} (t) versus ε_{Hf} (t) for Cenozoic volcanic rocks from the South China Sea (SCS) and the South China-Indochina continental margin (SCICM). See additional supporting information Data Set S1 for data sources. DMM = depleted MORB mantle; SCLM = subcontinental lithospheric mantle.

the amphibolite Kt9 (Figures 2 and 3). However, the samples Kt1 and Kt2 show variable enrichments in LREEs, LILEs, and Th-U relative to N-MORB (Figure 2). The unleached powders show high $^{87}Sr/^{86}Sr$ values, and the $^{143}Nd/^{144}Nd$ values of the leached Kt1 and Kt2 are higher than their unleached counterparts (Table S3). The Nd-Hf isotopes of the leached Kt1 and Kt2 are similar to those of the DMM end-member (Figure 3) and can be considered as primary signatures.

4.2. Basalts From the Miocene Spreading Ridge

The fresh cored MORB sample U1431 comprises mainly feldspar, clinopyroxene, and minor olivine with porphyroid texture (Figure S1). The sample has high content of SiO_2 (~52 wt. %) and low content of $K_2O + Na_2O$ (~3 wt. %) (Figure S2 and Table S2). LREEs are relative depleted ($[La/Yb]_N = 0.5$, N = chondrite normalized and hereinafter the same) and an N-MORB-like REE pattern is shown. The sample displays a positive Eu anomaly ($[Eu/Eu^*]_N = 1.5$) (Figure 2a) due to high contents of feldspar (Figure S1). However, LILEs (Cs, Rb, and Ba) and some high field strength elements (HFSEs, such as Th, U, Nb, Ta, Zr, Hf, and Ti) are significantly enriched relative to N-MORB (Figure 2b). The sample U1431 shows low $^{87}Sr/^{86}Sr$ (0.70302) high $^{143}Nd/^{144}Nd$ (0.51308) and $^{176}Hf/^{177}Hf$ (0.28314) and are more enriched as compared to the DMM end-member and the samples within the Kenting Mélange (Figure 3 and Table S3).

The basalt sample V36D9 from the Scarborough seamount chain has a porphyritic texture with small acicular feldspar phenocrysts (Figure S1). The rock shows low SiO_2 content (47.57 wt. %) and moderate concentration of $K_2O + Na_2O$ (3.9 wt. %) and exhibits feature of alkaline basalt (Figure S2 and Table S2). REE and incompatible element concentrations are similar to those of OIB, although somewhat depleted ($[La/Yb]_N = 5.3$; $(Dy/Yb)_N = 1.4$) relative to the OIB composition of Sun and McDonough (1989) (Figure 2). The seamount basalt V36D9 exhibits higher value of $^{87}Sr/^{86}Sr$ (0.70369), slightly lower $^{143}Nd/^{144}Nd$ (0.51291) and $^{176}Hf/^{177}Hf$ (0.28307) values compared with the ~16 Ma N-MORB samples from Site U1431 (Figure 3). However, sample V36D9 is slightly depleted with respect to the other seamount basalts from South China Sea (Figure 3).

5. Discussion

5.1. Depleted MORB-Like Mantle Fed the Late Oligocene Seafloor Spreading

Although seafloor metamorphism and weathering have altered the major elements (Figure S2), LILEs (Figure 2), and $^{87}Sr/^{86}Sr$ values (Figure 3a) of the samples from the Kenting Mélange, their HFSEs and

Nd-Hf isotopes remained relatively stable and can be used as reliable proxies to evaluate the mantle sources. The amphibolite Kt9 and basalt Kt5 from the Kenting Mélange show N-MORB-type chondrite-normalized REE patterns (Figure 2a) reflecting a depleted mantle and mid-ocean ridge-type tectonic setting. Furthermore, the ε_{Nd}(t) and ε_{Hf}(t) values of the samples from the Kenting Mélange are notably high with very limited variation, suggesting a DMM-like mantle source (Figure 3b). Therefore, we infer that these basaltic rocks might have been derived from the forearc spreading center of the Manila Trench, the Huatung Basin, and/or the South China Sea (Figure 1a).

The middle Miocene ophiolitic blocks in Lichi, eastern Taiwan (Figure 1b), are thought to be derived from the forearc spreading center of the Manila Trench (Shao, 2015). The Nd isotopic values of N-MORBs and gabbros of the ophiolite in Lichi (ε_{Nd} = 9.5–13.3; Jahn, 1986) are higher than those of the samples Kt1, Kt2, Kt5, and Kt9 in our study (ε_{Nd} = 7.5–9.3). The Cretaceous Huatung Basin is mainly composed of enriched MORB (E-MORB)-like oceanic crust (Hickey-Vargas et al., 2008). Although the Huatung MORBs display a large range of Nd-Hf isotopic values (ε_{Nd} = 6.8–9.9; ε_{Hf} = 14.5–23.1; Hickey-Vargas et al., 2008), the ε_{Hf} values at a given ε_{Nd} are higher than those of the amphibolite Kt9 and basalts Kt2 and Kt5. Most importantly, amphibolites within the Kenting Mélange yield late Oligocene U-Pb zircon (~25 Ma, X. Zhang et al., 2016) and K-Ar hornblende ages (~23–22 Ma, Pelletier & Stephan, 1986). Since zircon grains separated from the amphibolite Kt9 show faint oscillatory zoning patterns typical of igneous zircon (Hanchar & Miller, 1993), the U-Pb age is considered to represent the crystallization age of the gabbroic protolith (X. Zhang et al., 2016). The similar ages of crystallization and amphibolite-facies metamorphism indicate that amphibolites within the Kenting Mélange probably were generated by high-temperature metamorphism along ridge axis (Honnorez et al., 1984; Mevel, 1988). Consequently, the N-MORB type highly incompatible element patterns (Figure 2), the DMM-like Nd and Hf isotopic signatures (Figure 3b), and the late Oligocene ages of crystallization and metamorphism strongly suggest that the basaltic rocks within the Kenting Mélange are most likely crustal fragments of the South China Sea. Thus, the late Oligocene oceanic crust of the South China Sea might derive from a DMM-like mantle source.

However, the amphibolite Kt9 and basalts Kt5 and Kt2 display obvious negative Nb anomalies relative to other HFSEs (Figure 2b), which is similar to those of backarc basin basalt (BABB) in the West Philippine Basin (Hickey-Vargas, 1998; Savov et al., 2006). The distribution patterns of the Th, U, and LREEs of the sample Kt9 and Kt5 almost parallel those of the N-MORB standard, and the Th, U, and LREEs of the sample Kt9 and Kt5 are slightly depleted relative to their heavy REEs, Ti, and Y (Figure 2b). Accordingly, we argue that the negative Nb anomalies of the amphibolite Kt9 and basalt Kt5 would represent the original features rather than the selected enrichments of Th and U caused by metamorphism and weathering. Normally, the negative Nb anomaly of the BABB is caused by influx of subduction components into the DMM source (Pearce & Stern, 2006). Since the South China Sea developed upon the late Mesozoic Andean-type South China continental margin (Ru & Pigott, 1986; Taylor & Hayes, 1983), the BABB-like signatures of the amphibolite Kt9 and basalt Kt5 might be related to an earlier metasomatism of the DMM-like mantle caused by the Mesozoic subduction of the Paleo-Pacific Plate (section 5.3).

5.2. Mantle Enrichment and Upwelling of Hainan Plume During the Miocene

As shown in Figure 3, the Miocene MORBs and OIBs of the South China Sea are isotopically enriched progressively relative to those late Oligocene MORBs and this enrichment can be explained by a simple binary mixing model. OIB-type intraplate volcanism of the South China-Indochina continental margin and the South China Sea resurged since ~23.8 Ma (Figure 1a). Consequently, the ~16 Ma isotopically enriched MORBs of the South China Sea can be referred to Miocene influx of OIB-type components into the DMM-like mantle domain. In contrast, the less enriched seamount basalt V36D9 can be related to minor dilution of OIB-type enriched mantle source by MORB-like mantle components or responded to crustal contamination of rising OIB-type magma by MORBs. The basalt V36D9 shows strong negative Pb anomaly, which is contrast to other MORBs (Figure 2), indicating that crustal contamination from MORBs is negligible. It is widely acknowledged that the source mixing between the OIB-type components and the DMM-like mantle would couple with enriched incompatible elements. This is consistent with an occurrence of E-MORB rocks in the lower section of the core U1431 (G. L. Zhang & Jackson, 2016). Furthermore, the slightly enriched Nd-Hf isotopes of our N-MORB-type sample U1431 (Figure 3b) are coupled with the enrichments in LILEs (Cs, Rb, and Ba) and some HFSEs (such as Th, U, Nb, Ta, Zr, Hf, and Ti) (Figure 2b). However, other ~16 Ma MORB samples collected from the upper section of the core U1431 are N-MORBs but display more enriched Sr-Nd-Hf isotopes (G. L. Zhang et al., 2017) (Figure 3). Such elemental and isotopic decoupling reveals a special mantle process.

Similar isotopically enriched N-MORB rocks are common in oceanic ridge segments with large plume-ridge distances, and those elemental depleted but isotopically enriched sources are proposed to be decompression remelting of elementally depleted residue of plume materials (Yang et al., 2016). The existence of off-axis Hainan Plume has received support from increasing geophysical, petrologic, and geochemical evidence (Lei et al., 2009; X. C. Wang et al., 2012; Wang et al., 2013; S. Wei & Chen, 2016). Therefore, a possible petrogenesis of ~16 Ma isotopically enriched N-MORBs of the South China Sea is that the head of Hainan Plume have already arrived beneath the lithosphere since the early Miocene and the ridge suction (Y. G. Xu et al., 2012) introduced elementally depleted residue of plume materials into the mid-ocean ridge subsequently.

Alternatively, the Miocene influx of OIB-type components into the DMM-like mantle domain of the South China Sea can be referred to sporadic rising of hot and buoyant carbonated eclogite (G. L. Zhang et al., 2017) and the Miocene isotopically enriched N-MORBs could be formed in a shallow melting zone (G. L. Zhang & Jackson, 2016). However, such enriched mantle components including carbonated eclogite and garnet pyroxenite have been widely recognized in the source regions of late Cenozoic OIB-type intraplate volcanism of the South China-Indochina continental margin (Wang et al., 2013; Q. Yan et al., 2018; Zeng et al., 2017) and Miocene MORBs and OIBs of the South China Sea (G. L. Zhang & Jackson, 2016; G. L. Zhang et al., 2017). Subduction slabs, one of important sources of carbonated eclogite and garnet pyroxenite, have stayed in deep mantle beneath the South China-Indochina continental margin and the South China Sea since the early Mesozoic (Ru & Pigott, 1986; Shi & Li, 2012; Taylor & Hayes, 1983). Nevertheless, the elementally and isotopically depleted signatures of our late Oligocene MORBs indicate that the pervasive emergence of these long-lived enriched mantle components might generally focus on the late Cenozoic volcanism. We speculate that their upwelling might be relevant to a significant tectonothermal event (i.e., the upwelling of Hainan Plume).

Most importantly, it predicted that when a plume head impinged the lithosphere, the associated buoyancy would lift up its upper lithosphere and lead to local plate reorganization, such as ridge jump, increase of spreading rate, and enhanced propagation of an existing ridge system (Campbell, 2005; Hill, 1991). Furthermore, the onset of plume-deriving volcanism would be some of delayed 3–5 Ma after the arriving of plume head beneath lithosphere (Campbell, 2005). Therefore, the middle Oligocene (~28.5 Ma) significant uplift of the South China continental margin (Q. Li et al., 2005), the late Oligocene abrupt increase of spreading rate (C. F. Li et al., 2014), and the latest Oligocene/earliest Miocene ridge jump and ridge propagation (Briais et al., 1993; C. F. Li et al., 2014) were probably related to the middle Oligocene arriving of Hainan Plume head beneath the lithosphere of the South China continental margin. Moreover, ~23.8–20 Ma OIB-type intraplate volcanism outcropped in the South China Sea (X. Li et al., 2015) and the South China continental margin (X. L. Huang et al., 2013; K. L. Wang, Lo, et al., 2012) (Figure 1a) could be the earliest plume-deriving volcanism after a ~5 Ma arriving of plume head beneath the lithosphere.

5.3. Mantle Evolution Associated With the Opening of the South China Sea

It is well known that magmas with OIB features are not always the product of mantle plumes (Hawkesworth & Scherstén, 2007). For instance, the concomitant OIB-type and IAB-type volcanic rocks of the southern basin and range province of the United States are thought to be derived from decompression-related partial melting of asthenospheric upper mantle and continental mantle without the involvement of a mantle plume (Bradshaw et al., 1993). The continental margin of South China has been rifting since late Mesozoic when the Paleo-Pacific Plate subducted beneath it (Ru & Pigott, 1986; Taylor & Hayes, 1983). Such a tectonic environment is similar to that of the basin and range province (Gilder et al., 1991). Thus, Paleocene and Eocene OIB-type and IAB-type volcanic rocks of the South China continental margin (Figure 1a) might derive from the passively upwelling asthenosphere and the metasomatic South China subcontinental lithospheric mantle (SCLM) (X. L. Huang et al., 2013; K. L. Wang, Chung, et al., 2012).

Isotopically depleted mantle xenoliths of the late Cenozoic intraplate basalts (Tatsumoto et al., 1992; X. S. Xu et al., 2003) reveal that the depleted SCLM beneath the South China had been virtually replaced by the hot asthenosphere (X. S. Xu et al., 2000; Y. G. Xu et al., 2002). The replaced lower depleted SCLM should have been converted into the upper asthenospheric mantle and probably formed the source of ~25 Ma BABB-like

MORBs. Since slab dehydration and sediments melting are preferentially occurred at relatively shallow depths, the replaced South China lower SCLM would be less metasomatic than the upper SCLM counterpart. Hence, MORBs fed by this replaced lower SCLM would only show slightly negative Nb anomaly, and this is consistent with our ~25 Ma N-MORBs (Figure 2b). As soon as Hainan Plume flattened the base of lithosphere since the middle Oligocene, the asthenospheric mantle beneath the South China Sea would become progressively enriched due to influx of the plume material (Figure 3).

6. Conclusions

A progressive enrichment of the MORB mantle beneath the South China Sea during Miocene is identified. The ~25 Ma BABB-like MORB fragments of the late Miocene Kenting Mélange reveal a less metasomatic DMM-like source fed the late Oligocene seafloor spreading of the South China Sea. In contrast, the ~16 Ma elementally and isotopically enriched MORBs and ~9 Ma less enriched OIB-type seamount basalts from the South China Sea east subbasin indicate influx of an enriched asthenospheric source and possibly signal the contribution of the Hainan Plume. We conclude that MORBs which are relevant to progressive influx of the Hainan Plume components into the DMM-like source region of the South China Sea might appear since ~23.8 Ma following the middle Oligocene arriving of plume head beneath the lithosphere of the South China continental margin. On the contrary, the Paleocene and Eocene OIB-type volcanism in South China continental margin was derived from the passively upwelling of enriched asthenosphere due to continental rifting. The upwelling asthenosphere heated and replaced the ancient SCLM of South China, and partial melting of the upper highly metasomatic SCLM layer produced the Paleocene and Eocene IAB-type volcanism. Whereas, the lower less metasomatic depleted SCLM layer might have formed the DMM-like asthenospheric mantle source of the South China Sea.

Acknowledgments
We thank the Editor Jeroen Ritsema and two reviewers from the Journal for their valuable and constructive comments which significantly improved our paper. The data supporting the conclusions can be found in supporting information Tables S1–S3 and additional supporting information Data Set S1. Inspiration from Xiaolong Huang is gratefully acknowledged. We thank Guoliang Zhang for reading the manuscript and providing constructive suggestions. We are also grateful for samples shared by scientists from IODP Expedition 349, particular Zhen Sun, and for samples from the Lamont-Doherty Core Repository. This work was supported by the National Natural Science Foundation of China (41476036, U1505231, 41472093, U1701641, and 41676048). This is contribution IS-2509 from GIGCAS.

References

Bradshaw, T. K., Hawkesworth, C. J., & Gallagher, K. (1993). Basaltic volcanism in the Southern Basin and Range: No role for a mantle plume. *Earth and Planetary Science Letters*, *116*(1–4), 45–62. https://doi.org/10.1016/0012-821X(93)90044-A

Briais, A., Patriat, P., & Tapponnier, P. (1993). Updated interpretation of magnetic anomalies and seafloor spreading stages in the South China Sea: Implications for the Tertiary tectonics of Southeast Asia. *Journal of Geophysical Research*, *98*(B4), 6299–6328. https://doi.org/10.1029/92JB02280

Campbell, I. H. (2005). Large igneous provinces and the mantle plume hypothesis. *Elements*, *1*(5), 265–269. https://doi.org/10.2113/gselements.1.5.265

Chung, S. L., Cheng, H., Jahn, B. M., O'Reilly, S. Y., & Zhu, B. (1997). Major and trace element, and Sr-Nd isotope constraints on the origin of Paleogene volcanism in South China prior to the South China Sea opening. *Lithos*, *40*(2-4), 203–220. https://doi.org/10.1016/S0024-4937(97)00028-5

Chung, S. L., Jahn, B. M., Chen, S. J., Lee, T., & Chen, C. H. (1995). Miocene basalts in northwestern Taiwan: Evidence for EM-type mantle sources in the continental lithosphere. *Geochimica et Cosmochimica Acta*, *59*(3), 549–555. https://doi.org/10.1016/0016-7037(94)00360-X

Chung, S. L., Sun, S. S., Tu, K., Chen, C. H., & Lee, C. Y. (1994). Late Cenozoic basaltic volcanism around the Taiwan Strait, SE China: Product of lithosphere-asthenosphere interaction during continental extension. *Chemical Geology*, *112*(1-2), 1–20. https://doi.org/10.1016/0009-2541(94)90101-5

Gilder, S. A., Keller, G. R., Luo, M., & Goodell, P. (1991). Eastern Asia and the western Pacific timing and spatial distribution of rifting in China. *Tectonophysics*, *197*(2–4), 225–243. https://doi.org/10.1016/0040-1951(91)90043-R

Hanchar, J. M., & Miller, C. F. (1993). Zircon zonation patterns as revealed by cathodoluminescence and backscattered electron images: Implications for interpretation of complex crustal histories. *Chemical Geology*, *110*(1-3), 1–13. https://doi.org/10.1016/0009-2541(93)90244-D

Hawkesworth, C., & Scherstén, A. (2007). Mantle plumes and geochemistry. *Chemical Geology*, *241*(3-4), 319–331. https://doi.org/10.1016/j.chemgeo.2007.01.018

Hickey-Vargas, R. (1998). Origin of the Indian Ocean-type isotopic signature in basalts from Philippine Sea plate spreading centers: An assessment of local versus large-scale processes. *Journal of Geophysical Research*, *103*(B9), 20,963–20,979. https://doi.org/10.1029/98JB02052

Hickey-Vargas, R., Bizimis, M., & Deschamps, A. (2008). Onset of the Indian Ocean isotopic signature in the Philippine Sea Plate: Hf and Pb isotope evidence from Early Cretaceous terranes. *Earth and Planetary Science Letters*, *268*(3-4), 255–267. https://doi.org/10.1016/j.epsl.2008.01.003

Hill, R. I. (1991). Starting plumes and continental break-up. *Earth and Planetary Science Letters*, *104*(2–4), 398–416. https://doi.org/10.1016/0012-821X(91)90218-7

Ho, K. S., Chen, J. C., & Juang, W. S. (2000). Geochronology and geochemistry of late Cenozoic basalts from the Leiqiong area, southern China. *Journal of Asian Earth Sciences*, *18*(3), 307–324. https://doi.org/10.1016/S1367-9120(99)00059-0

Ho, K. S., Chen, J. C., Lo, C. H., & Zhao, H. L. (2003). ^{40}Ar–^{39}Ar dating and geochemical characteristics of late Cenozoic basaltic rocks from the Zhejiang–Fujian region, SE China: Eruption ages, magma evolution and petrogenesis. *Chemical Geology*, *197*(1-4), 287–318. https://doi.org/10.1016/S0009-2541(02)00399-6

Honnorez, J., Mével, C., & Montigny, R. (1984). Geotectonic significance of gneissic amphibolites from the Vema fracture zone, Equatorial Mid–Atlantic Ridge. *Journal of Geophysical Research*, *89*(B13), 11,379–11,400. https://doi.org/10.1029/JB089iB13p11379

Huang, X. L., Niu, Y., Xu, Y. G., Ma, J. L., Qiu, H. N., & Zhong, J. W. (2013). Geochronology and geochemistry of Cenozoic basalts from eastern Guangdong, SE China: Constraints on the lithosphere evolution beneath the northern margin of the South China Sea. *Contributions to Mineralogy and Petrology*, *165*(3), 437–455. https://doi.org/10.1007/s00410-012-0816-7

Huang, C. Y., Wu, W. Y., Chang, C. P., Tsao, S., Yuan, P. B., Lin, C. W., & Xia, K. Y. (1997). Tectonic evolution of accretionary prism in the arc-continent collision terrane of Taiwan. *Tectonophysics*, *281*(1–2), 31–51. https://doi.org/10.1016/S0040-1951(97)00157-1

Jahn, B. M. (1986). Mid-ocean ridge or marginal basin origin of the East Taiwan Ophiolite: Chemical and isotopic evidence. *Contributions to Mineralogy and Petrology*, *92*(2), 194–206. https://doi.org/10.1007/BF00375293

Lallemand, S., Font, Y., Bijwaard, H., & Kao, H. (2001). New insights on 3-D plates interaction near Taiwan from tomography and tectonic implications. *Tectonophysics*, *335*(3-4), 229–253. https://doi.org/10.1016/S0040-1951(01)00071-3

Le Bas, M. J., & Streckeisen, A. L. (1991). The IUGS systematics of igneous rocks. *Journal of the Geological Society*, *148*(5), 825–833. https://doi.org/10.1144/gsjgs.148.5.0825

Lebedev, S., & Nolet, G. (2003). Upper mantle beneath Southeast Asia from S velocity tomography. *Journal of Geophysical Research*, *108*(B1), 2048. https://doi.org/10.1029/2000JB000073

Lei, J., Zhao, D., Steinberger, B., Wu, B., Shen, F., & Li, Z. (2009). New seismic constraints on the upper mantle structure of the Hainan plume. *Physics of the Earth and Planetary Interiors*, *173*(1-2), 33–50. https://doi.org/10.1016/j.pepi.2008.10.013

Li, Q., Jian, Z., & Su, X. (2005). Late Oligocene rapid transformations in the South China Sea. *Marine Micropaleontology*, *54*(1-2), 5–25. https://doi.org/10.1016/j.marmicro.2004.09.008

Li, X. H., Li, Z. X., Wingate, M. T., Chung, S. L., Liu, Y., Lin, G. C., & Li, W. X. (2006). Geochemistry of the 755 Ma Mundine Well dyke swarm, northwestern Australia: Part of a Neoproterozoic mantle superplume beneath Rodinia? *Precambrian Research*, *146*(1-2), 1–15. https://doi.org/10.1016/j.precamres.2005.12.007

Li, X., Li, J., Yu, X., Wang, C., & Jourdan, F. (2015). ^{40}Ar/^{39}Ar ages of seamount trachytes from the South China Sea and implications for the evolution of the northwestern sub-basin. *Geoscience Frontiers*, *6*(4), 571–577. https://doi.org/10.1016/j.gsf.2014.08.003

Li, C. F., Xu, X., Lin, J., Sun, Z., Zhu, J., Yao, Y., et al. (2014). Ages and magnetic structures of the South China Sea constrained by deep tow magnetic surveys and IODP Expedition 349. *Geochemistry, Geophysics, Geosystems*, *15*, 4958–4983. https://doi.org/10.1002/2014GC005567

Liu, Y. (1996). Simultaneous and precise determination of 40 trace element elements using ICP-MS (in Chinese with English abstract). *Geochimica*, *25*, 552–558.

Liu, E., Wang, H., Uysal, I. T., Zhao, J. X., Wang, X. C., Feng, Y., & Pan, S. (2017). Paleogene igneous intrusion and its effect on thermal maturity of organic-rich mudstones in the Beibuwan Basin, South China Sea. *Marine and Petroleum Geology*, *86*, 733–750. https://doi.org/10.1016/j.marpetgeo.2017.06.026

Mevel, C. (1988). Metamorphism in oceanic layer 3, Gorringe Bank, eastern Atlantic. *Contributions to Mineralogy and Petrology*, *100*(4), 496–509. https://doi.org/10.1007/BF00371379

Morley, C. K. (2002). A tectonic model for the tertiary evolution of strike–slip faults and rift basins in SE Asia. *Tectonophysics*, *347*(4), 189–215. https://doi.org/10.1016/S0040-1951(02)00061-6

Pearce, J. A., & Stern, R. J. (2006). Origin of back-arc basin magmas: Trace element and isotope perspectives. In D. M. Christie, et al. (Eds.), *Back-arc spreading systems, geological, biological, chemical, and physical interactions, Geophysical Monograph Series* (Vol. 166, pp. 63–86). Washington, DC: American Geophysical Union. https://doi.org/10.1029/166GM06

Pelletier, B., & Stephan, J. F. (1986). Middle Miocene deduction and late Miocene beginning of collision registered in the hengchun peninsula: Geodynamic implications for the evolution of Taiwan. *Tectonophysics*, *125*(1–3), 133–160. https://doi.org/10.1016/0040-1951(86)90011-9

Ru, K., & Pigott, J. D. (1986). Episodic rifting and subsidence in the South China Sea. *AAPG Bulletin*, *70*(9), 1136–1155.

Savov, I. P., Hickey-Vargas, R., D'antonio, M., Ryan, J. G., & Spadea, P. (2006). Petrology and geochemistry of West Philippine Basin basalts and early Palau-Kyushu arc volcanic clasts from ODP Leg 195, Site 1201D: Implications for the early history of the Izu-Bonin-Mariana arc. *Journal of Petrology*, *47*(2), 277–299. https://doi.org/10.1093/petrology/egi075

Shao, W. Y. (2015). *Zircon U-Pb and Hf isotope constraints on the petrogenesis of igneous rocks in eastern Taiwan (Doctoral dissertation)* (in Chinese with English abstract). Taipei City: National Taiwan University.

Shi, H., & Li, C. F. (2012). Mesozoic and early Cenozoic tectonic convergence-to-rifting transition prior to opening of the South China Sea. *International Geology Review*, *54*(15), 1801–1828. https://doi.org/10.1080/00206814.2012.677136

Storey, B. C. (1995). The role of mantle plumes in continental breakup: Case histories from Gondwanaland. *Nature*, *377*(6547), 301–308. https://doi.org/10.1038/377301a0

Sun, S. S., & McDonough, W. S. (1989). Chemical and isotopic systematics of oceanic basalts: Implications for mantle composition and processes. *Geological Society of London, Special Publications*, *42*(1), 313–345. https://doi.org/10.1144/GSL.SP.1989.042.01.19

Tapponnier, P., Peltzer, G., Le Dain, A. Y., Armijo, R., & Cobbold, P. (1982). Propagating extrusion tectonics in Asia: New insights from simple experiments with plasticine. *Geology*, *10*(12), 611–616. https://doi.org/10.1130/0091-7613(1982)10%3C611:PETIAN%3E2.0.CO;2

Tatsumoto, M., Basu, A. R., Wankang, H., Junwen, W., & Guanghong, X. (1992). Sr, Nd, and Pb isotopes of ultramafic xenoliths in volcanic rocks of Eastern China: Enriched components EMI and EMII in subcontinental lithosphere. *Earth and Planetary Science Letters*, *113*(1–2), 107–128. https://doi.org/10.1016/0012-821X(92)90214-G

Taylor, B., & Hayes, D. E. (1983). Origin and history of the South China Sea basin. In D. E. Hayes (Ed.), *The tectonic and geologic evolution of Southeast Asian Seas and Islands: Part 2, Geophysical Monograph Series* (Vol. 27, pp. 23–56). Washington, DC: American Geophysical Union. https://doi.org/10.1029/GM027p0023

Tu, K., Flower, M. F., Carlson, R. W., Xie, G., Chen, C. Y., & Zhang, M. (1992). Magmatism in the South China Basin: 1. Isotopic and trace-element evidence for an endogenous Dupal mantle component. *Chemical Geology*, *97*(1–2), 47–63. https://doi.org/10.1016/0009-2541(92)90135-R

Wang, K. L., Chung, S. L., Lo, Y. M., Lo, C. H., Yang, H. J., Shinjo, R., et al. (2012). Age and geochemical characteristics of Paleogene basalts drilled from western Taiwan: Records of initial rifting at the southeastern Eurasian continental margin. *Lithos*, *155*, 426–441. https://doi.org/10.1016/j.lithos.2012.10.002

Wang, X. C., Li, Z. X., Li, X. H., Li, J., Liu, Y., Long, W. G., et al. (2012). Temperature, pressure, and composition of the mantle source region of Late Cenozoic basalts in Hainan Island, SE Asia: A consequence of a young thermal mantle plume close to subduction zones? *Journal of Petrology*, *53*(1), 177–233. https://doi.org/10.1093/petrology/egr061

Wang, X. C., Li, Z. X., Li, X. H., Li, J., Xu, Y. G., & Li, X. H. (2013). Identification of an ancient mantle reservoir and young recycled materials in the source region of a young mantle plume: Implications for potential linkages between plume and plate tectonics. *Earth and Planetary Science Letters*, *377-378*, 248–259. https://doi.org/10.1016/j.epsl.2013.07.003

Wang, K. L., Lo, Y. M., Chung, S. L., Lo, C. H., Hsu, S. K., Yang, H. J., & Shinjo, R. (2012). Age and geochemical features of dredged basalts from offshore SW Taiwan: The coincidence of intra-plate magmatism with the spreading South China Sea. *Terrestrial, Atmospheric & Oceanic Sciences*, *23*(6). https://doi.org/10.3319/TAO.2012.07.06.01(TT)

Wang, X. J., Wu, M. Q., Liang, D. H., & Yin, A. W. (1985). Some geochemical characteristics of basalts in the South China Sea. *Geochimica*, *4*(4), 380–390.

Wei, S. S., & Chen, Y. J. (2016). Seismic evidence of the Hainan mantle plume by receiver function analysis in southern China. *Geophysical Research Letters*, *43*, 8978–8985. https://doi.org/10.1002/2016GL069513

Wei, G., Liang, X., Li, X. H., & Liu, Y. (2002). Precise measurement of Sr isotopic composition of liquid and solid base using (LP) MC-ICPMS (in Chinese with English abstract). *Geochimica*, *31*(3), 295–299.

Weis, D., Kieffer, B., Maerschalk, C., Pretorius, W., & Barling, J. (2005). High-precision Pb-Sr-Nd-Hf isotopic characterization of USGS BHVO-1 and BHVO-2 reference materials. *Geochemistry, Geophysics, Geosystems*, *6*, Q02002. https://doi.org/10.1029/2004GC000852

Winchester, J. A., & Floyd, P. A. (1977). Geochemical discrimination of different magma series and their differentiation products using immobile elements. *Chemical Geology*, *20*, 325–343. https://doi.org/10.1016/0009-2541(77)90057-2

Xu, X. S., O'Reilly, S. Y., Griffin, W. L., & Zhou, X. (2000). Genesis of young lithospheric mantle in Southeastern China: An LAM–ICPMS trace element study. *Journal of Petrology*, *41*(1), 111–148. https://doi.org/10.1093/petrology/41.1.111

Xu, X. S., O'Reilly, S. Y., Griffin, W. L., & Zhou, X. (2003). Enrichment of upper mantle peridotite: Petrological, trace element and isotopic evidence in xenoliths from SE China. *Chemical Geology*, *198*(3-4), 163–188. https://doi.org/10.1016/S0009-2541(03)00004-4

Xu, Y. G., Sun, M., Yan, W., Liu, Y., Huang, X. L., & Chen, X. M. (2002). Xenolith evidence for polybaric melting and stratification of the upper mantle beneath South China. *Journal of Asian Earth Sciences*, *20*(8), 937–954. https://doi.org/10.1016/S1367-9120(01)00087-6

Xu, Y. G., Wei, J., Qiu, H., Zhang, H., & Huang, X. (2012). Opening and evolution of the South China Sea constrained by studies on volcanic rocks: Preliminary results and a research design. *Chinese Science Bulletin*, *57*(24), 3150–3164. https://doi.org/10.1007/s11434-011-4921-1

Yan, P., Deng, H., Liu, H., Zhang, Z., & Jiang, Y. (2006). The temporal and spatial distribution of volcanism in the South China Sea region. *Journal of Asian Earth Sciences*, *27*(5), 647–659. https://doi.org/10.1016/j.jseaes.2005.06.005

Yan, Q., Shi, X., & Castillo, P. R. (2014). The late Mesozoic-Cenozoic tectonic evolution of the South China Sea: A petrologic perspective. *Journal of Asian Earth Sciences*, *27*(5), 647–659. https://doi.org/10.1016/j.jseaes.2005.06.005

Yan, Q., Shi, X., Metcalfe, I., Liu, S., Xu, T., Kornkanitnan, N., et al. (2018). Hainan mantle plume produced late Cenozoic basaltic rocks in Thailand, Southeast Asia. *Scientific Reports*, *8*(1), 2640. https://doi.org/10.1038/s41598-018-20712-7

Yang, A. Y., Zhao, T. P., Zhou, M. F., & Deng, X. G. (2016). Isotopically enriched N-MORB: A new geochemical signature of off-axis plume-ridge interaction—A case study at 50° 28′ E, Southwest Indian Ridge. *Journal of Geophysical Research: Solid Earth*, *122*, 191–213. https://doi.org/10.1002/2016JB013284

Zeng, G., Chen, L. H., Yu, X., Liu, J. Q., Xu, X. S., & Erdmann, S. (2017). Magma-magma interaction in the mantle beneath eastern China. *Journal of Geophysical Research: Solid Earth*, *122*, 2763–2779. https://doi.org/10.1002/2017JB014023

Zhang, X., Cawood, P. A., Huang, C. Y., Wang, Y., Yan, Y., Santosh, M., et al. (2016). From convergent plate margin to arc-continent collision: Formation of the Kenting Mélange, Southern Taiwan. *Gondwana Research*, *38*, 171–182. https://doi.org/10.1016/j.gr.2015.11.010

Zhang, G. L., Chen, L. H., Jackson, M. G., & Hofmann, A. W. (2017). Evolution of carbonated melt to alkali basalt in the South China Sea. *Nature Geoscience*, *10*(3), 229–235. https://doi.org/10.1038/NGEO2877

Zhang, G. L., & Jackson, M. G. (2016). *Geochemical constraints on mantle source and melting dynamics of the South China Sea spreading center*. Paper presented at the 2016 American Geophysical Union Fall Meeting, San Francisco, California.

Zhang, X., Yan, Y., Huang, C. Y., Chen, D., Shan, Y., Lan, Q., et al. (2014). Provenance analysis of the Miocene accretionary prism of the Hengchun Peninsula, southern Taiwan, and regional geological significance. *Journal of Asian Earth Sciences*, *85*, 26–39. https://doi.org/10.1016/j.jseaes.2014.01.021

Zhou, H., Xiao, L., Dong, V., Wang, C., Wang, F., & Ni, P. (2009). Geochemical and geochronological study of the Sanshui basin bimodal volcanic rock suite, China: Implications for basin dynamics in southeastern China. *Journal of Asian Earth Sciences*, *34*(2), 178–189. https://doi.org/10.1016/j.jseaes.2008.05.001

Zhu, B. Q., Wang, H. F., Chen, Y. W., Chang, X. Y., Hu, Y. G., & Xie, J. (2004). Geochronological and geochemical constraint on the Cenozoic extension of Cathaysian lithosphere and tectonic evolution of the border sea basins in East Asia. *Journal of Asian Earth Sciences*, *24*(2), 163–175. https://doi.org/10.1016/j.jseaes.2003.10.006

Zou, H. P., Li, P., & Rao, C. (1995). Geochemistry of Cenozoic volcanic rocks in Zhujiangkou basin and its geodynamic significance (in Chinese with English abstract). *Geochimica*, *S1*.

Zou, H. B., Zindler, A., Xu, X., & Qi, Q. (2000). Major, trace element, and Nd, Sr and Pb isotope studies of Cenozoic basalts in SE China: Mantle sources, regional variations, and tectonic significance. *Chemical Geology*, *171*(1-2), 33–47. https://doi.org/10.1016/S0009-541(00)00243-6